MRI in mouse models of brain disorders

Istvan Pirko, MD

Istvan Pirko, MD
Senior Associate Consultant
Department of Neurology
Associate Professor of Neurology
College of Medicine
Phone: 507-538-1039
Secretary: 507-284-4458
Fax: 507-266-4419
E-mail: pirko@mayo.edu

_____

Mayo Clinic
200 First Street SW
Rochester, MN 55905
www.mayoclinic.org

Introduction

Animal models are frequently used in the study of complex human diseases. These disease models represent selected aspects or occasionally the full spectrum of the corresponding human disease. Complex diseases of the nervous system, including vascular, inflammatory, neoplastic and neurodegenerative diseases are commonly studied in murine models. Mouse colonies are relatively easy to maintain, and the wide availability of transgenic animals coupled with the capability of generating new, genetically modified mice from well characterized "standard" strains represents a major advantage in identifying and exploring molecular pathogenic mechanisms relevant to the given condition.

One of the most common ways to approach research questions in biomedical sciences is to visualize tissue compartments or cellular interactions in various tissues. Standard optical microscopy-based techniques allow for studies of ex vivo tissue with high resolution and with a varying degree of specificity depending on the staining method used. Newer intravital microscopy techniques are also emerging and have become very useful tools in monitoring cellular motion and cell-cell interactions. Since most disease processes are dynamic, non-invasive in vivo imaging modalities are of great advantage as they allow for investigations at multiple different time points. MRI investigations in mice allow for translational projects – the radiological features known to accompany human diseases can often be modeled and studied in details. The first manuscript describing MR imaging of a rat was published over 30 years ago.[2] MRI has the capability of studying live organisms without exposing them to potentially harmful ionizing radiation. Besides anatomical imaging, MRI is also capable of providing physiological information about several important aspects of biological processes. These include circulation and cerebrospinal fluid (CSF) flow, cerebral blood volume distribution, activity mapping with fMRI or Mn^{++} based techniques, metabolite distribution with chemical shift imaging, diffusion or perfusion properties of the studied tissue, or in vivo pH measurement via phosphorous MRS.

Technical aspects of small animal MR imaging

Many universities and research institutions now own small animal MRI imaging systems, most commonly as part of a core facility. Most facilities use 4-16 Tesla narrow bore magnets; with 7 Tesla becoming the most common option. The two leading manufacturers of these systems are Bruker Biospin (Ettlingen, Germany) and Varian Medical Systems, Inc (Palo Alto, CA). Both vertical and horizontal bore systems are available. Usually, in facilities run by biochemists, vertical bore NMR spectrometers equipped with gradient coils and imaging probes are used; whereas in facilities run by MRI physicists or radiologists, horizontal bore magnets are more common. Obviously, the physical principles remain the same regardless of orientation of the bore; however, horizontal bore system often allow for easier monitoring of the mice and larger flexibility in customizing the probes and coils. Most facilities employ their own engineers and technicians. Larger facilities often develop not only their own pulse sequences and post-processing software tools, but also design their own hardware, including RF coils and rodent head stabilizing probes. Although most commonly only the field strength is mentioned when discussing the differences between imaging systems; however, the utilized coils are

equally important, and can literally make or break the success of a CNS MRI research program. Custom made coils specific to the studied research question often have significantly better SNR than stock coils.

While MR image acquisition is a very complex process in and of itself, image analysis is often far more time consuming and computation intense process than acquisition. Some image processing and visualization tools generally are included with the scanner manufacturers' software, but they are generally insufficient to provide the desired detailed answers. Several commercially available biomedical image post-processing software packages are available and many research institutions develop their own software applications for this purpose. Notable examples of image analysis software are Analyze [3, 4], SPM [5] the freely downloadable NIH image (http://rsb.info.nih.gov/nih-image/)[6][6][6], or AFNI (http://afni.nimh.nih.gov/). Most of these provide basic analysis methods including intensity, ROI-based surface or volume measurements; they also include tools for slice extraction from 3D volumes, and for a variety of 3D visualizations. Several offer segmentation, coregistration, and tools for complex analysis requiring image algebra methods, including DTI visualization, perfusion calculations, or fMRI visualization tools.

Special requirements for small rodent MR imaging

MRI requires the study subjects to be completely immobilized, and the importance of this can't be stressed enough. In order to achieve this goal, general anesthesia must be used in small animal experiments.[7] In most cases, this means inhalational anesthesia. Unlike injectable agents, inhalational anesthesia is administered continuously, and can be calibrated to the specific requirements posed by the animal and the experiment. The investigators need to be aware that the anesthesia may in some cases alter the desired imaging outcome; this is especially true for cerebral blood volume and functional MRI studies.[8] In most cases, animal monitoring while under anesthesia is an important requirement. This includes monitoring of core temperature, respiratory rate and ECG. This is also important from the standpoint of gated acquisition, which is often needed in an effort to eliminate respiration or cardiac motion-related artifacts during acquisition. The most commonly used systems are manufactured by SA Instruments, Inc (Stony Brook, NY; http://www.i4sa.com/).

The core temperature inside narrow-bore scanners can easily be in the low 50 °F range (15-20 °C). Various heating system are utilized in an effort to maintain the normal core temperature of the animals while in the scanner. These are usually supplied by the vendors of the imaging systems directly.
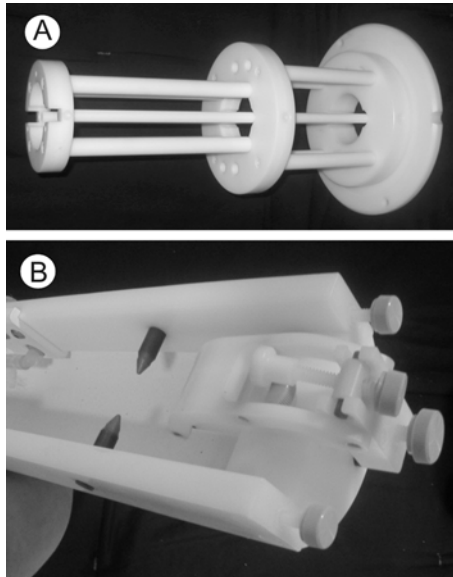
FIG. 1. Custom designed mouse probe. Mounting plane (A) custom designed for 20 cm bore MRI. Stereotaxic device (B) showing ear and teeth bars plus gas anesthetic supply and scavenging lines.[9]

Besides the anesthesia and maintaining a suitable core temperature, another important factor is that probe should keep the animal stable during the imaging session.[7, 8, 10] Most small animal systems are shipped with mouse and rat probes, but many labs develop custom-made holders for specific applications (FIG.1). A good probe will achieve maximal stabilization without any trauma to the animal. Ideally, probes should allow for easily reproducible stereotactic placement.

Differences between small animal imaging and human MRI: advantages and disadvantages of higher field strength

It is important to understand that the study of experimental animals with MRI differs in more ways than just the smaller scale that rodent imaging requires; however, the smaller scale itself is a major problem to overcome (FIG. 2.) Most animal magnets operate at high field strength, in the range of 4-16 Tesla, as opposed to the standard clinical scanners in the 1.5-3 Tesla range. The relaxation properties are different at this field strength. The SAR or specific absorption rate becomes a key limiting factor at higher field strength for in vivo experiments; novel pulse sequences may be required to overcome the limitations this poses. Lower flip angle or higher TR may need to be used to allow for image acquisition without potentially dangerous energy absorption and related heating of the tissue, however, these parameters obviously have a major influence on image contrast.

FIG. 2. Extracted brain and spinal cord of a SJL/J mouse. The entire mouse brain is about the size of the caudate nucleus in a human brain.

Most investigators would like to obtain image sets of excellent resolution and high SNR in a very little time. It is important to recognize that each of the above three component (SNR, resolution, imaging time) are interdependent. For example, the price one pays for a good SNR is frequently a lower resolution and/or longer acquisition time. Or, if both good SNR and resolution are the goals, then the imaging time usually needs to be prolonged. Finding an acceptable balance may be a difficult task; several parameters of the studied model should be considered when trying to optimize image acquisition.

Living organisms can be considered inhomogeneous samples, with compartmentalized organs. Gaseous, solid, and various consistencies of liquid (from fluid to gelatinous) substances can be found in living organisms. These different consistencies have different magnetic susceptibilities, and while this in general does not represent a major problem at lower field strength, it becomes a very important problem at the higher field strength used in small animal imaging and MRI microscopy. Magnetic susceptibility is a known source of artifacts. One of the best known is the loss of brain signal near air-filled sinuses. Gradient echo based sequences are especially prone to these artifacts. It can also interfere with fat suppression and diffusion experiments. Several methods have been proposed to reduce these artifacts, including the GESEPI sequence.[11, 12] In GE imaging, slice selection correction methods have also been tried and successfully used.[13, 14] For spin echo multislice studies, the use of phase-phase encoding was found helpful in reducing susceptibility related artifacts. Variants of fast spin echo (FSE) or RARE (rapid acquisition relaxation enhancement) [15] sequences use RF refocused echoes, which eliminate or reduce much of the susceptibility-related artifacts.

It should also be noted that in some applications, susceptibility-related artifacts might be of benefit. Iron oxide based negative contrast agents (small or ultra small superparamagnetic iron oxide particles or (U)SPIO-s) are detectable through their property of generating strong susceptibility effects. Since susceptibility artifacts are stronger at high field strength, these contrast materials are especially

suitable for small animal imaging. Susceptibility weighted imaging or SWI is another novel method that takes advantage of this issue, and represents a novel tissue contrast [16, 17].

MRI of the central nervous system in small animal models

Several neurological disease models have been studied with small animal MRI. One of the most basic applications is to generate *3D anatomical atlases of rodent brains*. This has been accomplished by several groups.[18-21] Similarly, MRI atlases describing mouse embryonic development have also been generated and reported.[22] A web-based application assembled by the California Institute of Technology allows insight into one of these databases.[23][23][23] Examples of in vivo and ex vivo anatomical imaging is shown on FIGs. 3 and 4 [9].
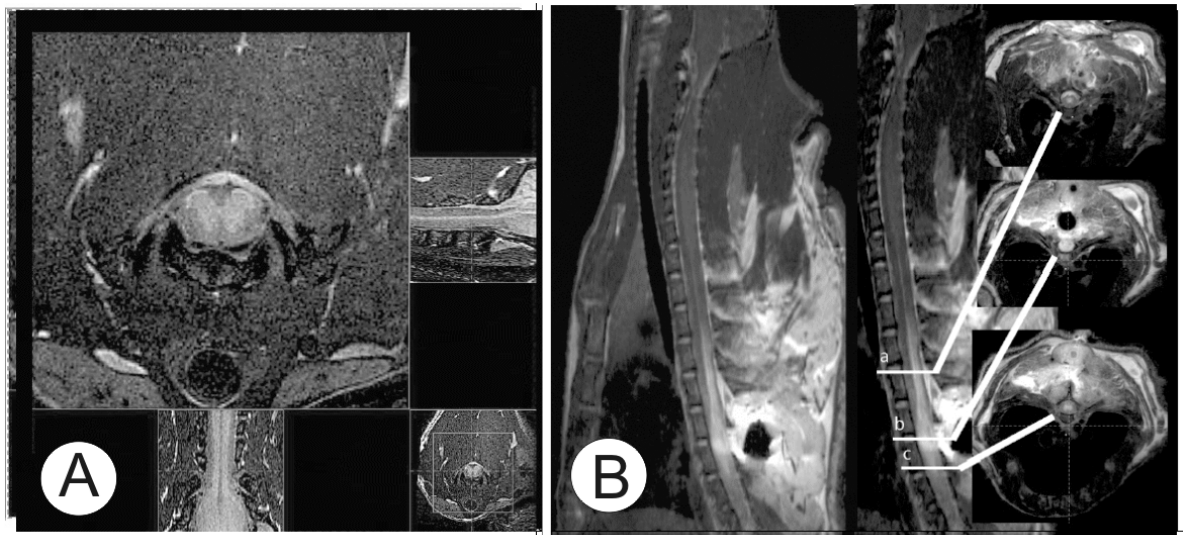

FIG. 3. . A) Anatomical imaging of rat spinal cord in vivo. Note the excellent delineation between gray and white matter. B) In vivo rat cord, T2 weighted study. Spinal cord injury is clearly shown on sagittal image, also on axial cuts (a-c) at different levels across the lesion. [9]

In basic neuroscience research, *tract tracing via MRI* is an important and as of yet under-utilized application. This technique utilizes paramagnetic Mn^{++} ions. Neurons pass the Mn^{++} ions to each other via the synaptic junctures, thus allowing visualization of neural pathways by MRI.[24-27] It is believed that Mn^{++} ions enter the cells due to receptor activated calcium channel opening. Once inside the cell, Mn^{++} ions utilize axonal microtubule transport mechanisms to get to the axon terminal. During synaptic transmission, Mn^{++} is released from the pre-synaptic neuron. It is able to enter the post-synaptic neuron via calcium channels.[25] Thus Mn^{++} will accumulate in activated chains of neurons, leading to increased signal intensity in activated parts of the CNS. If applied topically to parts of the cortex, to olfactory neurons, or to the retina, Mn^{++} can be used for tract tracing. While this technique requires invasive administration of this novel contrast material, the possibility of in vivo tract tracing is in itself a remarkable achievement. An example for MEMRI is shown on Figure 5 [28]
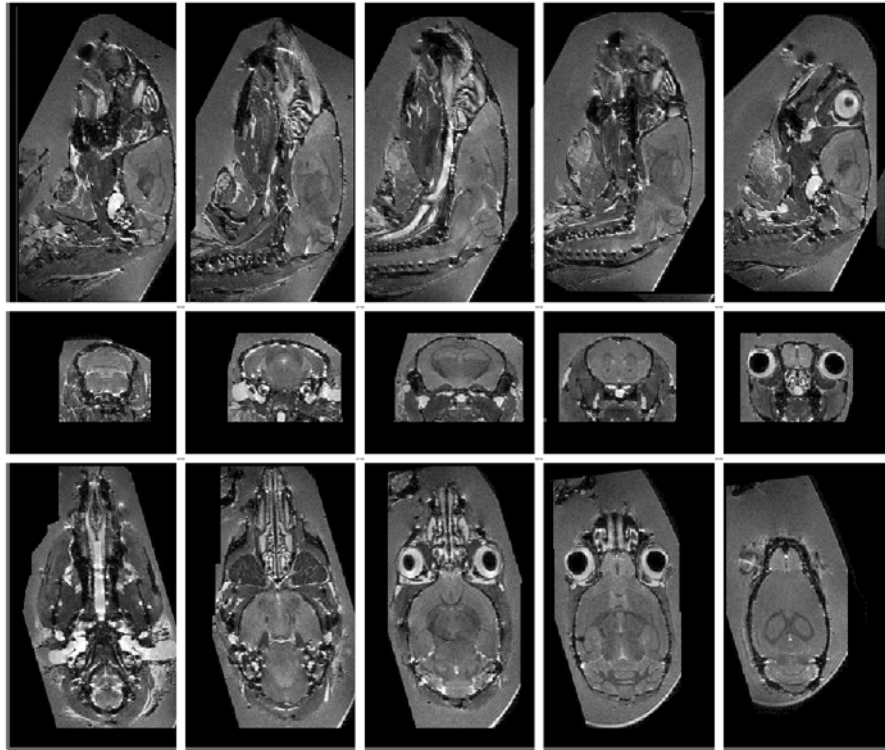
FIG. 4. 7 Tesla (300 MHz) MR microscopy of ex vivo mouse head. Note excellent anatomical resolution of sagittal (top) coronal (middle) and axial (bottom row) images extracted from a 3D dataset. The high SNR and high isotropic resolution (100 μm/pixel) are achieved at the expense of long scanning time (33 h). Other parameters: FOV 51.2×25.6×25.6 mm^3, matrix size 512×256×256, TR 1.8 s, TE 50 ms.[9]

Functional MRI studies can also be conducted in small rodents. fMRI studies are based on the blood oxygen level dependent (BOLD) principle. Blood flow and oxy/deoxy-hemoglobin related changes in activated areas of the cortex produce mild hypointensity on T2* images. [29, 30]'[31, 32] . Images obtained in the activated and non-activated state can be used to generate activity maps, including sensory or visual cortex mapping in animals.[31, 33] One potential limitation shown by several studies is that inhaled anesthetics may alter the signal. Also, mild hypocapnia may be helpful in establishing BOLD contrast. Some rodent fMRI studies also utilized SPIO/USPIO contrast materials to enhance signal loss at the activated areas,[32] these techniques also allow the measurement of cerebral blood volume.[32, 34, 35]
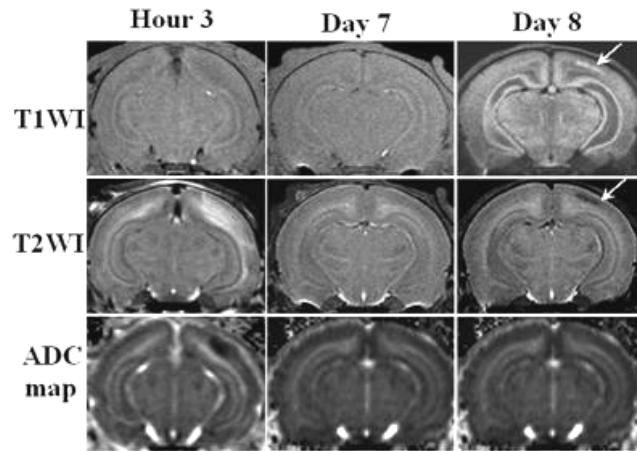
Figure 5. Typical gray matter lesion in a rat model of hypoxic-ischemic injury (arrows in T1WI and T2WI) was observed in late phase by MEMRI after Mn2+ injection in Day 7, which was not visible in the T2WI, T1WI and ADC map [28].

Inflammatory diseases of the CNS are frequently studied in animal models. The most common models include experimental allergic encephalomyelitis (EAE), Theiler's Murine Encephalitis Virus infection (TMEV) and toxic demyelination models. Similar to human diseases, lesion formation can be monitored by T2 weighted sequences (FIG.6.).
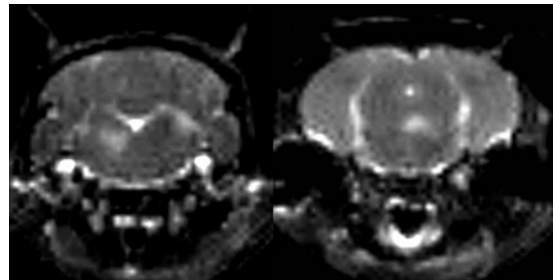

FIG. 6. Demyelinating lesions in interferon-γ receptor knockout mice following Theiler's virus infection. Note the high signal intensity areas in the brainstem and near the thalamus on these T2 weighted in vivo images. [9]

Gadolinium enhancement can be used to monitor the blood-brain barrier permeability associated with new lesion formation.[36] Atrophy measurements become important for the chronic aspects of these diseases, volumetric MRI techniques based on 3D acquisition sequences [36, 37] are key components in the study of brain atrophy. Diffusion weighted imaging (DWI) is also important in these models, since this technique may show lesion formation even earlier than gadolinium contrast imaging.[38] By the use of diffusion tensor imaging (DTI) methods, tract integrity can also be studied.[39] Voxel based MR spectroscopy (MRS, see below) or chemical shift imaging studies are also used, mainly to assess axonal integrity and membrane turnover.[37, 40]

Cell specific and molecular imaging studies are now used in the study of several disease models.[41-43] In the near future, a surge of these techniques is expected, as the correlation between conventional histology and MRI methods is best achieved by the use of these tools. Several groups have reported

8

success with immune cell-specific imaging, utilizing superparamagnetic contrast materials (SPIO and USPIO) that are either internalized by cells after ex vivo incubation, or bound to the cells by specific antibodies [41, 43-47] (FIG. 6.). Another potential application of similar USPIO-based labeling techniques is to follow the distribution of biologically active proteins.[41]
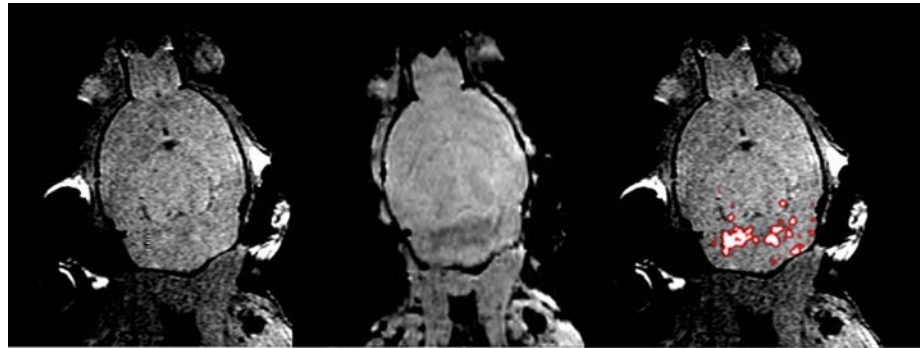

FIG. 6. CD8+ T-cell labeling with USPIO conjugated antibodies in Theiler's encephalitis virus infection. Left image: T1 weighted study shows faint hyperintense areas in cerebellum. Middle image: T2* weighted image shows hypointensities in cerebellum. Right image: composite image, using a mask generated by dividing the T1 weighted image matrix with the T2* weighted[9]

Optic neuritis is an inflammatory demyelinating disease affecting the second cranial nerve. It can represent a standalone disease, but is also a common component of MS and NMO. Due to the uniformity of the ON fibers, animal models of ON can be studied using advanced MRI methods. (Figure 7)[48].
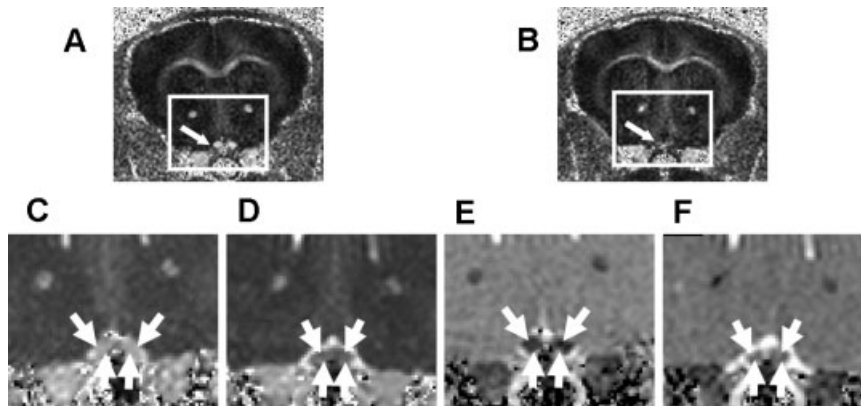

FIG. 7. Optic nerves (indicated by arrows) from the EAE-affected mouse appear hypointense (B) in RA (relative anisotropy) maps compared with the control (A). Decreased axial diffusivity (D) and increased radial diffusivity (F) in optic nerves from EAE-affected mice were observed in the expanded views of axial (C and D) and radial diffusivity (E and F) corresponding to the rectangles in (A) and (B).[48]

Iron deposition as a component in the pathology of neurodegenerative diseases can also be studied by MRI. This is even seen in certain MS models, as recently reported by our team of investigators(Figure 8.) [49]. Since iron is known to cause susceptibility-related artifacts and high fields strength imaging is more prone to those artifacts (see above), small animal MRI is very suitable to study this phenomenon.[50]
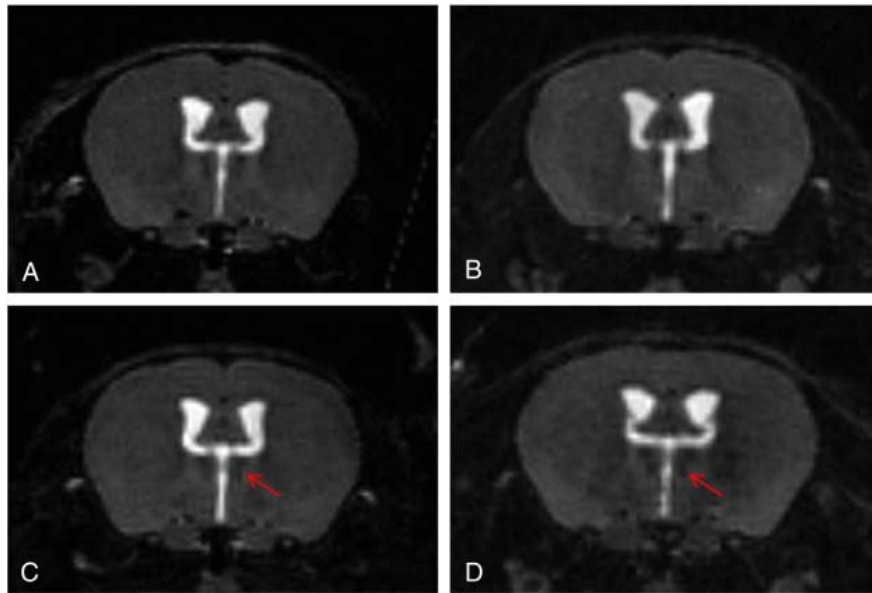

FIG. 8. Example of progressive thalamic T2 hypointensity in a virally induced MS model at 1 (A), 4 (B), 6 (C) and 12 (D) months post disease induction. A–D represent coronal slices extracted from the original 3D datasets. Note the hypointensity of the medio-dorsal thalamic nucleus and the increasing hypointensity at the later time points (arrows).

In the study of *neurodegenerative disease models*, morphometric studies can be used for atrophy measurements. Both global brain atrophy measurements as well as focal volume loss of brain structures can be assessed using MRI.[50-53] One example is the recently reported cerebellar cortical atrophy in an EAE model. [49]

Alzheimer's pathology has been very difficult to study with MRI. However, through the use of novel contrast agents, one group has reported good success in imaging Alzheimer plaques ex vivo.[54, 55] More recently, even without contrast agents, plaque imaging in small rodent models has become possible both ex vivo[56] and in vivo (Figure 9)[57].[58][57][57]
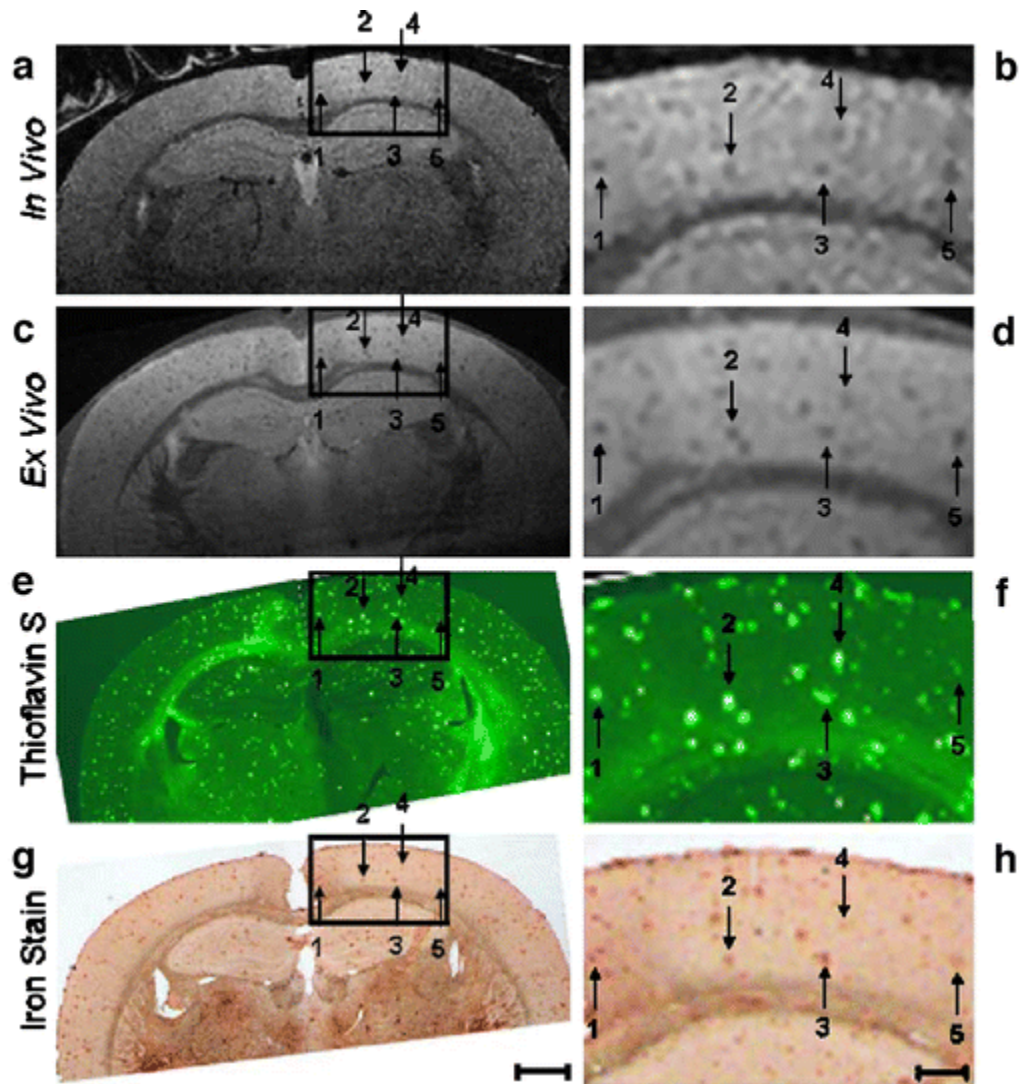
FIG. 9. 12-month-old AD mouse. In vivo (**a**, **b**) and ex vivo (**c**, **d**) T_2SE-weighted MR images, Thioflavin-S-stained (**e**, **f**) and iron-stained (**g**, **h**) histological brain sections have been precisely spatially registered over a circumscribed area of the cortex, indicated by the *box*. The *boxes* in the *right column* (*scale bar*, 100 μm) represent 3× magnified portions of the adjacent parent image in the *left column* (*scale bar*, 1.0 mm). The *numbered arrows* indicate individual plaques visualized in each of the four different image types that matched with the linked-cursor system.   [57]

MRS studies are also frequently used in the study of neurodegenerative diseases, mainly to assess axonal pathology by studying the NAA (N-acetyl aspartate) peak.[59] Phosphorous MRS studies can also be used to study energy metabolites[60][59][59].

Experimental stroke models in small rodents are frequently studied with MRI methods. These generally require classic MR imaging modalities, including T1, T2 and proton density imaging. Newer techniques include the use of diffusion and perfusion imaging, also MRS for determining certain metabolites.[61, 62] Many groups have used experimental MCA ligation combined with hypoxia in rats or mice as

11

models for human stroke.[63] DWI sequences are especially powerful in detecting early ischemia, and many studies have utilized this resource in animal imaging, along with perfusion studies that are capable of visualizing the penumbra – the area at risk for infarction that potentially can be salvaged (FIG. 10). [62, 64]
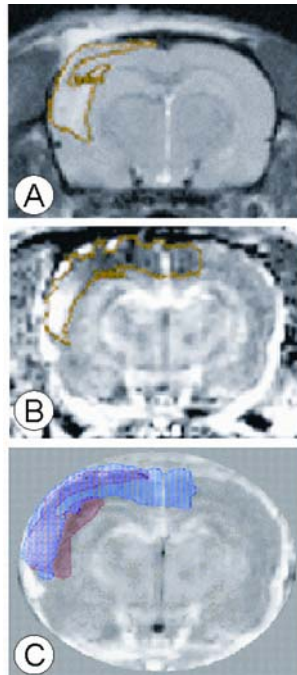

FIG. 10. Diffusion and perfusion weighted MRI studies in a rodent model. (A) diffusion weighted image; (B) perfusion image; (C) diffusion-perfusion mismatch. The area of diffusion-perfusion mismatch is thought to represent potentially salvageable areas in stroke and brain injury models. [9]

When DTI is done with a fast imaging sequence like EPI, the temporal resolution of scanning can be as low as every 20-30 seconds/entire brain scan, allowing close monitoring of stroke development. MRS studies have also been conducted, mainly looking at the lactate peak, which becomes prominent when anaerobic glycolysis predominates.[61, 62, 65] Another important aspect is the NAA peak, that may show decrease in completed strokes, but may remain normal if the animals still can recover from the ischemic event.[66] MRA[67] and CBV/CBF studies [34] have been done and evaluated in several stroke models. These studies can accurately characterize the blood flow and blood volume during ischemia.

Several models of *brain trauma* have been developed in experimental animals. These range from diffuse injuries to controlled cortical impacts, chemical insult, non-impact models. MRI allows monitoring of the damaged tissue, also the tissue at risk.[10, 68, 69] For this purpose DWI/DTI/MT (magnetization transfer) techniques are often used, similarly to stroke studies described above (FIG. 11.) MR spectroscopy is also utilized for the study of tissue injury in the CNS (FIG. 12.). [70, 71]
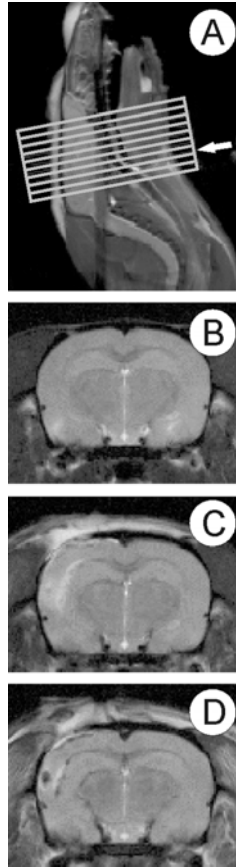
FIG. 11. Diffusion weighted longitudinal imaging time course study of rat brain prior to and following traumatic brain injury. Sagittal slice (A) showing position of coronal slices. Coronal slice (B) prior to injury; (C) coronal slice 24 hours after injury; (D) 96 hours after injury. Images C and D were obtained without the use of scout images and without the use of slice localization, by utilizing a stereotactic probe designed at Georgetown University (FIG. 1.)[9]

FIG. 12. . *In vivo* spectra from left and right side of rat brain following traumatic brain injury. A single 8 µl voxel was positi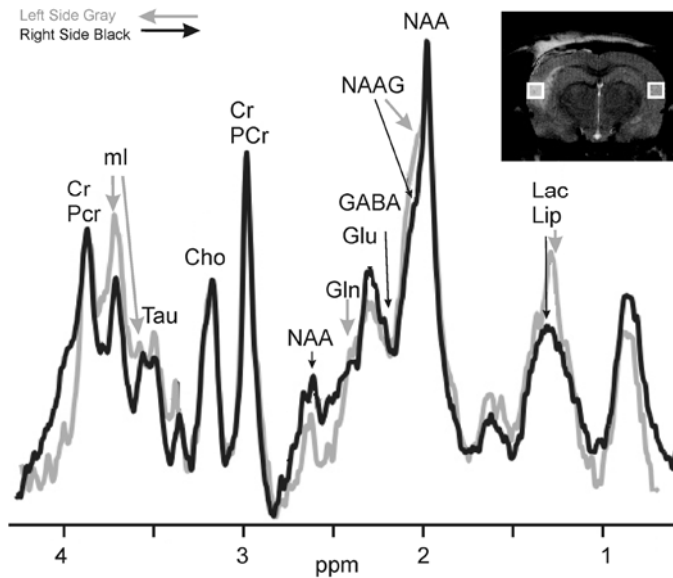oned on lesion and another on the contralateral side. Differences in Lactate, Glutamate, NAAG, NAA and myo-inositol are evident on in-vivo MRS.

Animal models of *brain tumors* are also frequently studied by MRI and MRS (FIG. 13.).[72]'[73, 74] The basic T1 and T2 weighted techniques may not always allow an obvious delineation between healthy and tumor infiltrated tissue; advanced MRI methods and cell labeling techniques may allow for the identification of transplanted tumor cells and may enable monitoring of their growth and expansion.
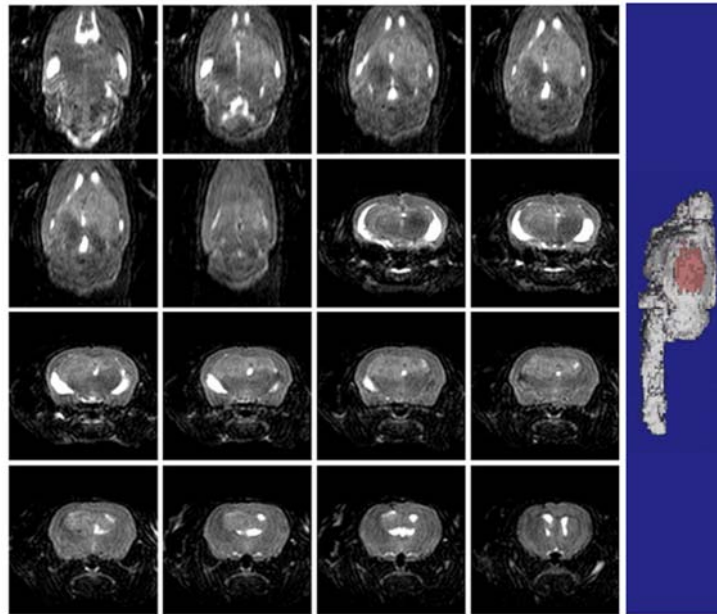

FIG. 13. Brain tumor imaging in nude mouse[75][74][74]. Left panel: T2 weighted in vivo dataset showing tumor growth on axial and coronal images. Note infiltrating tumor mass in thalamus and basal ganglia. Right panel: semitransparent 3D rendering of the same dataset. Using advanced post-processing methods, the 3D dataset was segmented based on the signal characteristics from healthy brain tissue vs. tumor infiltrated tissue.[9]

The use of intravenous contrast materials may show blood brain barrier breakdown in certain tumor models; also MRS studies (proton and phosphorous) can be used to study biochemical differences between cancerous and normal tissue in vivo. Diffusion and perfusion studies, along with blood flow and blood oxygen level dependent studies [76][75][75] may also provide useful information, since tumor cells generally show increased metabolism.

Conclusion

Over the last several years, microscopic resolution in vivo MRI has become a popular and versatile tool in the study of CNS diseases. MR image resolution of tens of microns in all three dimensions can now be achieved for in vivo studies, but for most practical application, an isometric resolution of approximately 100 micron appears to be sufficient. Because of the obstacles encountered with

physiological microscopic movements of tissues due to circulation, breathing, fluid flow, significantly higher resolutions are probably unrealistic for in vivo applications. Small animal MRI research is an important translational research tool in the study of CNS diseases. New developments from the fields of NMR and clinical MRI research both find their way to small animal experimental MRI research. Since a growing number of human CNS diseases have MRI-based diagnostic criteria, translational MRI research utilizing rodent models allows insight into important substrates of tissue dysfunction related to these clinically relevant MRI findings. The increased versatility that microscopic resolution MRI provides will lead to an enhanced understanding of critically important biological processes, and will likely result in the development of new diagnostic and treatment approaches in a variety of human CNS diseases.

References

1. Yang, J., et al., *Manganese-enhanced MRI detection of neurodegeneration in neonatal hypoxic-ischemic cerebral injury.* Magn Reson Med, 2008. **59**(6): p. 1329-39.
2. Hansen, G., et al., *In vivo imaging of the rat anatomy with nuclear magnetic resonance.* Radiology, 1980. **136**(3): p. 695-700.
3. Robb, R.A., *The virtualization of medicine: a decade of pitfalls and progress.* Stud Health Technol Inform, 2002. **85**: p. 1-7.
4. Robb, R.A., *3-D visualization in biomedical applications.* Annu Rev Biomed Eng, 1999. **1**: p. 377-99.
5. Turner, R., et al., *Functional magnetic resonance imaging of the human brain: data acquisition and analysis.* Exp Brain Res, 1998. **123**(1-2): p. 5-12.
6. *http://rsb.info.nih.gov/nih-image/Default.html.*
7. Lukasik, V.M. and R.J. Gillies, *Animal anaesthesia for in vivo magnetic resonance.* NMR Biomed, 2003. **16**(8): p. 459-67.
8. Kannurpatti, S.S. and B.B. Biswal, *Effect of anesthesia on CBF, MAP and fMRI-BOLD signal in response to apnea.* Brain Res, 2004. **1011**(2): p. 141-7.
9. Pirko, I., et al., *Magnetic resonance imaging, microscopy, and spectroscopy of the central nervous system in experimental animals.* NeuroRx, 2005. **2**(2): p. 250-64.
10. Fricke, S.T., et al., *Consistent and reproducible slice selection in rodent brain using a novel stereotaxic device for MRI.* J Neurosci Methods, 2004. **136**(1): p. 99-102.
11. Yang, Q.X., et al., *Removal of local field gradient artifacts in T2*-weighted images at high fields by gradient-echo slice excitation profile imaging.* Magn Reson Med, 1998. **39**(3): p. 402-9.
12. Yang, Q.X., et al., *Multiple echo frequency-domain image contrast: improved signal-to-noise ratio and T2 (T2*) weighting.* Magn Reson Med, 1999. **41**(2): p. 423-8.
13. Ordidge, R.J., et al., *Assessment of relative brain iron concentrations using T2-weighted and T2*-weighted MRI at 3 Tesla.* Magn Reson Med, 1994. **32**(3): p. 335-41.
14. Frahm, J., K.D. Merboldt, and W. Hanicke, *Direct FLASH MR imaging of magnetic field inhomogeneities by gradient compensation.* Magn Reson Med, 1988. **6**(4): p. 474-80.
15. Hennig, J. and H. Friedburg, *Clinical applications and methodological developments of the RARE technique.* Magn Reson Imaging, 1988. **6**(4): p. 391-5.
16. Haacke, E.M., *Susceptibility weighted imaging (SWI).* Z Med Phys, 2006. **16**(4): p. 237.
17. Haacke, E.M., et al., *Susceptibility-weighted imaging: technical aspects and clinical applications, part 1.* AJNR Am J Neuroradiol, 2009. **30**(1): p. 19-30.
18. Jacobs, R.E., et al., *MRI: volumetric imaging for vital imaging and atlas construction.* Nat Rev Mol Cell Biol, 2003. **Suppl**: p. SS10-6.
19. Dhenain, M., S.W. Ruffins, and R.E. Jacobs, *Three-dimensional digital mouse atlas using high-resolution MRI.* Dev Biol, 2001. **232**(2): p. 458-70.
20. MacKenzie-Graham, A., et al., *A multimodal, multidimensional atlas of the C57BL/6J mouse brain.* J Anat, 2004. **204**(2): p. 93-102.
21. Kovacevic, N., et al., *A Three-dimensional MRI Atlas of the Mouse Brain with Estimates of the Average and Variability.* Cereb Cortex, 2004.
22. Jacobs, R.E., et al., *Towards a microMRI atlas of mouse development.* Comput Med Imaging Graph, 1999. **23**(1): p. 15-24.
23. *http://mouseatlas.caltech.edu.*

24.   Pautler, R.G., R. Mongeau, and R.E. Jacobs, *In vivo trans-synaptic tract tracing from the murine striatum and amygdala utilizing manganese enhanced MRI (MEMRI).* Magn Reson Med, 2003. **50**(1): p. 33-9.

25.   Pautler, R.G. and A.P. Koretsky, *Tracing odor-induced activation in the olfactory bulbs of mice using manganese-enhanced magnetic resonance imaging.* Neuroimage, 2002. **16**(2): p. 441-8.

26.   Hu, T.C., et al., *Manganese-enhanced MRI of mouse heart during changes in inotropy.* Magn Reson Med, 2001. **46**(5): p. 884-90.

27.   Pautler, R.G., A.C. Silva, and A.P. Koretsky, *In vivo neuronal tract tracing using manganese-enhanced magnetic resonance imaging.* Magn Reson Med, 1998. **40**(5): p. 740-8.

28.   Yang, J. and E.X. Wu, *Manganese-enhanced MRI detected the gray matter lesions in the late phase of mild hypoxic-ischemic injury in neonatal rat.* Conf Proc IEEE Eng Med Biol Soc, 2007. **2007**: p. 51-4.

29.   Malisza, K.L. and P.W. Stroman, *Functional imaging of the rat cervical spinal cord.* J Magn Reson Imaging, 2002. **16**(5): p. 553-8.

30.   Malisza, K.L., et al., *Functional MRI of the rat lumbar spinal cord involving painful stimulation and the effect of peripheral joint mobilization.* J Magn Reson Imaging, 2003. **18**(2): p. 152-9.

31.   Bock, C., et al., *Functional MRI of somatosensory activation in rat: effect of hypercapnic up-regulation on perfusion- and BOLD-imaging.* Magn Reson Med, 1998. **39**(3): p. 457-61.

32.   Mandeville, J.B., et al., *Dynamic functional imaging of relative cerebral blood volume during rat forepaw stimulation.* Magn Reson Med, 1998. **39**(4): p. 615-24.

33.   Brinker, G., et al., *Simultaneous recording of evoked potentials and T2*-weighted MR images during somatosensory stimulation of rat.* Magn Reson Med, 1999. **41**(3): p. 469-73.

34.   Wu, E.X., et al., *High-resolution in vivo CBV mapping with MRI in wild-type mice.* Magn Reson Med, 2003. **49**(4): p. 765-70.

35.   Mandeville, J.B., et al., *Regional sensitivity and coupling of BOLD and CBV changes during stimulation of rat brain.* Magn Reson Med, 2001. **45**(3): p. 443-7.

36.   Pirko, I., et al., *Dynamics of MRI lesion development in an animal model of viral-induced acute progressive CNS demyelination.* Neuroimage, 2004. **21**(2): p. 576-82.

37.   Pirko, I., et al., *Disappearing "T1 black holes" in an animal model of multiple sclerosis.* Front Biosci, 2004. **9**: p. 1222-7.

38.   Heide, A.C., et al., *Diffusion imaging of experimental allergic encephalomyelitis.* Magn Reson Med, 1993. **29**(4): p. 478-84.

39.   Ahrens, E.T., et al., *MR microscopy of transgenic mice that spontaneously acquire experimental allergic encephalomyelitis.* Magn Reson Med, 1998. **40**(1): p. 119-32.

40.   Schwarcz, A., et al., *Localized proton MRS of cerebral metabolite profiles in different mouse strains.* Magn Reson Med, 2003. **49**(5): p. 822-7.

41.   Pirko, I., et al., *A human antibody that promotes remyelination enters the CNS and decreases lesion load as detected by T2-weighted spinal cord MRI in a virus-induced murine model of MS.* Faseb J, 2004. **18**(13): p. 1577-9.

42.   Pirko, I., et al., *In vivo magnetic resonance imaging of immune cells in the central nervous system with superparamagnetic antibodies.* Faseb J, 2004. **18**(1): p. 179-82.

43.   Pirko, I., et al., *Magnetic resonance imaging of immune cells in inflammation of central nervous system.* Croat Med J, 2003. **44**(4): p. 463-8.

44.   Bulte, J.W. and D.L. Kraitchman, *Iron oxide MR contrast agents for molecular and cellular imaging.* NMR Biomed, 2004. **17**(7): p. 484-99.

45. Bulte, J.W., et al., *Preparation of magnetically labeled cells for cell tracking by magnetic resonance imaging.* Methods Enzymol, 2004. **386**: p. 275-99.

46. Bulte, J.W., et al., *MR microscopy of magnetically labeled neurospheres transplanted into the Lewis EAE rat brain.* Magn Reson Med, 2003. **50**(1): p. 201-5.

47. Anderson, S.A., et al., *Magnetic resonance imaging of labeled T-cells in a mouse model of multiple sclerosis.* Ann Neurol, 2004. **55**(5): p. 654-9.

48. Xu, J., et al., *Assessing optic nerve pathology with diffusion MRI: from mouse to human.* NMR Biomed, 2008. **21**(9): p. 928-40.

49. Pirko, I., et al., *Deep gray matter T2 hypointensity correlates with disability in a murine model of MS.* J Neurol Sci, 2009. **282**(1-2): p. 34-8.

50. Gilissen, E.P., et al., *Topographical localization of iron in brains of the aged fat-tailed dwarf lemur (Cheirogaleus medius) and gray lesser mouse lemur (Microcebus murinus).* Am J Primatol, 1998. **45**(3): p. 291-9.

51. Lee, W.T. and C. Chang, *Magnetic resonance imaging and spectroscopy in assessing 3-nitropropionic acid-induced brain lesions: an animal model of Huntington's disease.* Prog Neurobiol, 2004. **72**(2): p. 87-110.

52. Choi, I.Y., et al., *In vivo NMR studies of neurodegenerative diseases in transgenic and rodent models.* Neurochem Res, 2003. **28**(7): p. 987-1001.

53. McDaniel, B., et al., *Tracking brain volume changes in C57BL/6J and ApoE-deficient mice in a model of neurodegeneration: a 5-week longitudinal micro-MRI study.* Neuroimage, 2001. **14**(6): p. 1244-55.

54. Poduslo, J.F., et al., *Molecular targeting of Alzheimer's amyloid plaques for contrast-enhanced magnetic resonance imaging.* Neurobiol Dis, 2002. **11**(2): p. 315-29.

55. Poduslo, J.F., et al., *Design and chemical synthesis of a magnetic resonance contrast agent with enhanced in vitro binding, high blood-brain barrier permeability, and in vivo targeting to Alzheimer's disease amyloid plaques.* Biochemistry, 2004. **43**(20): p. 6064-75.

56. Zhang, J., et al., *Detection of amyloid plaques in mouse models of Alzheimer's disease by magnetic resonance imaging.* Magn Reson Med, 2004. **51**(3): p. 452-7.

57. Jack, C.R., Jr., et al., *Magnetic resonance imaging of Alzheimer's pathology in the brains of living transgenic mice: a new tool in Alzheimer's disease research.* Neuroscientist, 2007. **13**(1): p. 38-48.

58. Jack, C.R., Jr., et al., *In vivo visualization of Alzheimer's amyloid plaques by magnetic resonance imaging in transgenic mice without a contrast agent.* Magn Reson Med, 2004. **52**(6): p. 1263-71.

59. Dedeoglu, A., et al., *Magnetic resonance spectroscopic analysis of Alzheimer's disease mouse brain that express mutant human APP shows altered neurochemical profile.* Brain Res, 2004. **1012**(1-2): p. 60-5.

60. Andjus, R.K., et al., *Brain energetics and tolerance to anoxia in deep hypothermia.* Annals of NY Academy of Sciences, 2005. **In press**.

61. Hesselbarth, D., et al., *High resolution MRI and MRS: a feasibility study for the investigation of focal cerebral ischemia in mice.* NMR Biomed, 1998. **11**(8): p. 423-9.

62. Hoehn, M., et al., *Application of magnetic resonance to animal models of cerebral ischemia.* J Magn Reson Imaging, 2001. **14**(5): p. 491-509.

63. Hata, R., et al., *A reproducible model of middle cerebral artery occlusion in mice: hemodynamic, biochemical, and magnetic resonance imaging.* J Cereb Blood Flow Metab, 1998. **18**(4): p. 367-75.

64. Xue, R., et al., *In vivo three-dimensional reconstruction of rat brain axonal projections by diffusion tensor imaging.* Magn Reson Med, 1999. **42**(6): p. 1123-7.

65. Dreher, W., et al., *Temporal and regional changes during focal ischemia in rat brain studied by proton spectroscopic imaging and quantitative diffusion NMR imaging.* Magn Reson Med, 1998. **39**(6): p. 878-88.

66. Malisza, K.L., et al., *Metabolite changes in neonatal rat brain during and after cerebral hypoxia-ischemia: a magnetic resonance spectroscopic imaging study.* NMR Biomed, 1999. **12**(1): p. 31-8.

67. Beckmann, N., *High resolution magnetic resonance angiography non-invasively reveals mouse strain differences in the cerebrovascular anatomy in vivo.* Magn Reson Med, 2000. **44**(2): p. 252-8.

68. Goetz, P., et al., *Increase in apparent diffusion coefficient in normal appearing white matter following human traumatic brain injury correlates with injury severity.* J Neurotrauma, 2004. **21**(6): p. 645-54.

69. Stoffel, M., et al., *Identification of brain tissue necrosis by MRI: validation by histomorphometry.* J Neurotrauma, 2004. **21**(6): p. 733-40.

70. Schuhmann, M.U., et al., *Metabolic changes in the vicinity of brain contusions: a proton magnetic resonance spectroscopy and histology study.* J Neurotrauma, 2003. **20**(8): p. 725-43.

71. Schuhmann, M.U., et al., *Long-time in-vivo metabolic monitoring following experimental brain contusion using proton magnetic resonance spectroscopy.* Acta Neurochir Suppl, 2002. **81**: p. 209-12.

72. Phuong, L.K., et al., *Use of a vaccine strain of measles virus genetically engineered to produce carcinoembryonic antigen as a novel therapeutic agent against glioblastoma multiforme.* Cancer Res, 2003. **63**(10): p. 2462-9.

73. Hirakawa, K., et al., *The investigation of experimental brain tumours using 31P-MRS and 1H-MRI.* Acta Neurochir Suppl (Wien), 1988. **43**: p. 140-4.

74. Gyngell, M.L., et al., *Proton MR spectroscopy of experimental brain tumors in vivo.* Acta Neurochir Suppl (Wien), 1994. **60**: p. 350-2.

75. Giannini, C., et al., *Patient Tumor EGFR and PDGFRA Gene Amplifications Retained in an Invasive Intracranial Xenograft Model of GBM.* Neuro-Oncology, 2005. **In press**.

76. Howe, F.A., et al., *Issues in flow and oxygenation dependent contrast (FLOOD) imaging of tumours.* NMR Biomed, 2001. **14**(7-8): p. 497-506.